THE JOURNAL OF PHYSICAL CHEMISTRY B

 VOLUME 105, NUMBER 19, MAY 17, 2001

LETTERS

EPR Study of the Semiquinone Biradical $Q_A^{\bullet-}Q_B^{\bullet-}$ in Photosynthetic Reaction Centers of *Rhodobacter sphaeroides* at 326 GHz: Determination of the Exchange Interaction J_o

Rafael Calvo,[†,‡] Roger A. Isaacson,[†] Mark L. Paddock,[†] Edward C. Abresch,[†] Melvin Y. Okamura,[†] Anna-Lisa Maniero,[§,#] Louis-Claude Brunel,[§] and George Feher*[,†]

Department of Physics, University of California, San Diego, 9500 Gilman Drive, La Jolla, Caifornia 92093-0319, Departamento de Física, Facultad de Bioquímica y Ciencias Biológicas, Universidad Nacional del Litoral, and INTEC (CONICET-UNL), Güemes 3450, 3000 Santa Fe, Argentina, and Center for Interdisciplinary Magnetic Resonance, National High Magnetic Field Laboratory, Florida State University, Tallahassee, Florida 32310

Received: January 23, 2001; In Final Form: March 21, 2001

The magnitude of the exchange interaction J_o, defined by $H_{exch} = -J_o\mathbf{S}_A\cdot\mathbf{S}_B$, between unpaired spins $\mathbf{S}_A$ and $\mathbf{S}_B$ in biological molecules is an important parameter in calculating electron-transfer rates. In a previous work, we obtained an approximate value of J_o for the biradical $Q_A^{\bullet-}Q_B^{\bullet-}$, which forms an intermediate state in the photocycle of reaction centers (RCs) of the photosynthetic bacterium *Rhodobacter sphaeroides* (Calvo, R. et al. *J. Am. Chem. Soc.* **2000**, *122*, 7327). In that work J_o was derived from EPR measurements at 35 and 94 GHz, frequencies at which the EPR spectra are relatively insensitive to J_o. In this work we obtained EPR spectra between 5 and 80 K at 326 GHz, a frequency at which the spectrum is more sensitive to J_o. Consequently, we were able to improve the accuracy of J_o approximately by an order of magnitude. From a global fit with a spin-Hamiltonian of the spectra at five temperatures we obtained a value of $J_o/h = (-82 \pm 3)$ MHz. The value of J_o is within the experimental uncertainty of the previously reported value and results in an estimated maximum electron-transfer rate between the semiquinones of $k_{ET}^{max} \approx 10^9\ s^{-1}$.

Introduction

In a recent paper[1] we reported the trapping and characterization of the semiquinone biradical $Q_A^{\bullet-}Q_B^{\bullet-}$, which forms an intermediate state in the photocycle of the bacterial photosynthetic reaction center (RC) from *Rhodobacter sphaeroides*.[2] EPR studies of frozen solutions of this biradical at 9.6, 35, and 94 GHz allowed us to determine an accurate value of the dipole−dipole interaction and to estimate the exchange interaction J_o between the radicals $Q_A^{\bullet-}$ and $Q_B^{\bullet-}$. From the dipolar interaction of the biradical, structural information (distance and angles) was obtained from the data. The structural results were in good agreement with the X-ray results obtained for the $D^+Q_AQ_B^{\bullet-}$ intermediate state of the photocycle.[3] The magnitude J_o of the exchange interaction is related to the electronic structure of the path connecting the unpaired spins in the biradical. The experimentally determined value of J_o was used to estimate a

* To whom correspondence should be addressed. Tel.: (858) 534-4389. Fax: (858) 822-0007. E-mail: gfeher@physics.ucsd.edu.
[†] University of California, San Diego.
[‡] Universidad Nacional del Litoral and CONICET.
[§] Florida State University.
[#] Permanent address: Dipartimento di Chimica Fisica, Università di Padova, I35131, Padova, Italy.

10.1021/jp0102670 CCC: $20.00
Published on Web 04/19/2001

maximum electron-transfer rate for the reaction $Q_A^{\bullet-}Q_B^{\bullet-} \rightarrow Q_AQ_B^{2-}$, using a simple model relating the matrix element for the exchange interaction with that for electron transfer.[1] However, the accuracy of the exchange interaction J_o calculated from our previous multifrequency EPR study was relatively poor (~30%). The reason is the insensitivity of the EPR spectrum of the biradical to the value of J_o when the difference between the Zeeman splitting of the two radicals, $|\Delta g|\mu_B B$, is smaller than $|J_o|$ (Δg is the difference between the g-factors g_A and g_B of $Q_A^{\bullet-}$ and $Q_B^{\bullet-}$, μ_B is the Bohr magneton, and B is the applied magnetic field). In our case, the principal values of the **g**-tensors of $Q_A^{\bullet-}$ and $Q_B^{\bullet-}$ are almost identical, and the principal axes are nearly collinear. Therefore, even at a microwave frequency of 94 GHz,[1] $|\Delta g|\mu_B B \ll |J_o|$, and the spectrum was relatively insensitive to J_o. As pointed out by the Eatons (S. S. Eaton and G. R. Eaton, (1994), High Field EPR Workshop, National High Magnetic Field Laboratory, Tallahassee, FL, unpublished) at higher frequencies several transitions can be observed that facilitate the determination of J_o. In the present work we obtained a more accurate value of J_o from EPR spectra of the biradical at 326 GHz, a frequency at which $|\Delta g|\mu_B B$ becomes larger and more comparable to $|J_o|$. From an analysis of the spectra a value of J_o was obtained that is approximately 1 order of magnitude more accurate than the value reported earlier.[1] Thus, this paper represents an extension of our previous work[1] to which the reader is referred for details, including relevant references. A preliminary account of this work has been reported.[4]

EPR Results

EPR spectra of $Q_A^{\bullet-}$ and $Q_A^{\bullet-}Q_B^{\bullet-}$, produced in RCs of *Rb. sphaeroides* as previously described,[1] were obtained at 326 GHz with an experimental setup described by Hassan et al.[5] They are displayed in Figure 1, with the peak-to-peak amplitudes normalized to the same value. Figure 1a displays the spectrum of the semiquinone $Q_A^{\bullet-}$ observed at 5 K. The shape of this spectrum does not change with temperature. In contrast, the spectrum of $Q_A^{\bullet-}Q_B^{\bullet-}$ varies with temperature, as shown in Figure 1b. The spectra exhibit additional peaks that are not observed in the $Q_A^{\bullet-}$ spectrum, nor had they been observed at 94 GHz. The relative amplitudes of some of the peaks decrease with decreasing temperature (see solid arrows in Figure 1b), the relative amplitude of other peaks do not vary with temperature (dashed arrows in Figure 1b). The temperature dependence of the amplitudes of the peaks enables us to identify the associated transitions, as discussed later.

Theory

The spin-Hamiltonian describing the energies of the four spin states of the biradical is[1]

$$H = \mu_B \mathbf{B}\cdot\mathbf{g}_A\cdot\mathbf{S}_A + \mu_B \mathbf{B}\cdot\mathbf{g}_B\cdot\mathbf{S}_B - J_o \mathbf{S}_A\cdot\mathbf{S}_B + E_d\{\mathbf{S}_A\cdot\mathbf{S}_B - 3(\mathbf{S}_A\cdot\rho)(\mathbf{S}_B\cdot\rho)\} \quad (1)$$

where **B** is the applied magnetic field, $\mathbf{g}_A$ and $\mathbf{g}_B$ are the **g**-tensors of the spins $\mathbf{S}_A$ and $\mathbf{S}_B$ on $Q_A^{\bullet-}$ and $Q_B^{\bullet-}$, respectively, and μ_B is the Bohr magneton. The first two terms are the Zeeman interaction of $Q_A^{\bullet-}$ and $Q_B^{\bullet-}$ ($S = {}^1/_2$). J_o is the magnitude of the exchange interaction. $E_d = g^2\mu_B{}^2/R^3$ is the magnitude of the dipole−dipole interaction between $\mathbf{S}_A$ and $\mathbf{S}_B$ in the point dipole approximation, and $\rho = \mathbf{R}/|\mathbf{R}|$ is a unit vector connecting the centers of $Q_A^{\bullet-}$ and $Q_B^{\bullet-}$. The dipolar term contains information about the distance R and the orientation ρ of the translation vector connecting $Q_A^{\bullet-}$ and $Q_B^{\bullet-}$.

The energies of the four eigenstates Ψ_i ($i = 1, ...,4$) of the Hamiltonian (eq 1), and the four allowed EPR transitions ($j =$ I, ...,IV) between these states are shown in Figure 2a. By diagonalizing eq 1 the field positions B_j of the resonances are obtained:[1]

I $\quad \Psi_1 \leftrightarrow \Psi_3$ at

$$B_I = B_o + \frac{J_o - d(\mathbf{h})}{\mu_B(g_A(\mathbf{h}) + g_B(\mathbf{h}))} - \frac{[\mu_B{}^2(g_A(\mathbf{h}) - g_B(\mathbf{h}))^2 B_I{}^2 + (J_o + {}^1/_2 d(\mathbf{h}))^2]^{1/2}}{\mu_B(g_A(\mathbf{h}) + g_B(\mathbf{h}))} \quad (2a)$$

II $\quad \Psi_1 \leftrightarrow \Psi_2$ at

$$B_{II} = B_o + \frac{J_o - d(\mathbf{h})}{\mu_B(g_A(\mathbf{h}) + g_B(\mathbf{h}))} + \frac{[\mu_B{}^2(g_A(\mathbf{h}) - g_B(\mathbf{h}))^2 B_{II}{}^2 + (J_o + {}^1/_2 d(\mathbf{h}))^2]^{1/2}}{\mu_B(g_A(\mathbf{h}) + g_B(\mathbf{h}))} \quad (2b)$$

III $\quad \Psi_3 \leftrightarrow \Psi_4$ at

$$B_{III} = B_o - \frac{J_o - d(\mathbf{h})}{\mu_B(g_A(\mathbf{h}) + g_B(\mathbf{h}))} + \frac{[\mu_B{}^2(g_A(\mathbf{h}) - g_B(\mathbf{h}))^2 B_{III}{}^2 + (J_o + {}^1/_2 d(\mathbf{h}))^2]^{1/2}}{\mu_B(g_A(\mathbf{h}) + g_B(\mathbf{h}))} \quad (2c)$$

IV $\quad \Psi_2 \leftrightarrow \Psi_4$ at

$$B_{IV} = B_o - \frac{J_o - d(\mathbf{h})}{\mu_B(g_A(\mathbf{h}) + g_B(\mathbf{h}))} - \frac{[\mu_B{}^2(g_A(\mathbf{h}) - g_B(\mathbf{h}))^2 B_{IV}{}^2 + (J_o + {}^1/_2 d(\mathbf{h}))^2]^{1/2}}{\mu_B(g_A(\mathbf{h}) + g_B(\mathbf{h}))} \quad (2d)$$

where $B_o = 2h\nu/\{\mu_B(g_A(\mathbf{h}) + g_B(\mathbf{h}))\}$ is the average field of the spectrum for a given orientation $\mathbf{h} = \mathbf{B}/|\mathbf{B}|$ of the applied magnetic field, $g_A(\mathbf{h})$ and $g_B(\mathbf{h})$ are the projections of the tensors $\mathbf{g}_A$ and $\mathbf{g}_B$ along **h**, and $d(\mathbf{h}) = E_d(1 - 3\cos^2\eta)$, where η is the angle between ρ and **h**. The transition probabilities P_j of these resonances are

$$P_I = P_{III} = |\langle\Psi_1|S_{A+} + S_{B+}|\Psi_3\rangle|^2 = 1 - \sin(2\alpha) \quad (3a)$$

$$P_{II} = P_{IV} = |\langle\Psi_1|S_{A+} + S_{B+}|\Psi_2\rangle|^2 = 1 + \sin(2\alpha) \quad (3b)$$

where α is defined by

$$\tan\alpha = \frac{-(J_o + {}^1/_2 d(\mathbf{h}))}{\mu_B(g_A(\mathbf{h}) - g_B(\mathbf{h}))B + [\mu_B{}^2(g_A(\mathbf{h}) - g_B(\mathbf{h}))^2 B^2 + (J_o + {}^1/_2 d(\mathbf{h}))^2]^{1/2}} \quad (4)$$

Positions and transition probabilities of the resonances depend on the orientation **h** of the applied magnetic field. The values for a given **h** can be calculated without approximations in terms of the spin-Hamiltonian parameters using eqs 2 and 3. A convolution over all field orientations has to be made to obtain the contribution of each of the four transition for randomly oriented RCs in a frozen solution sample. The spectrum of the

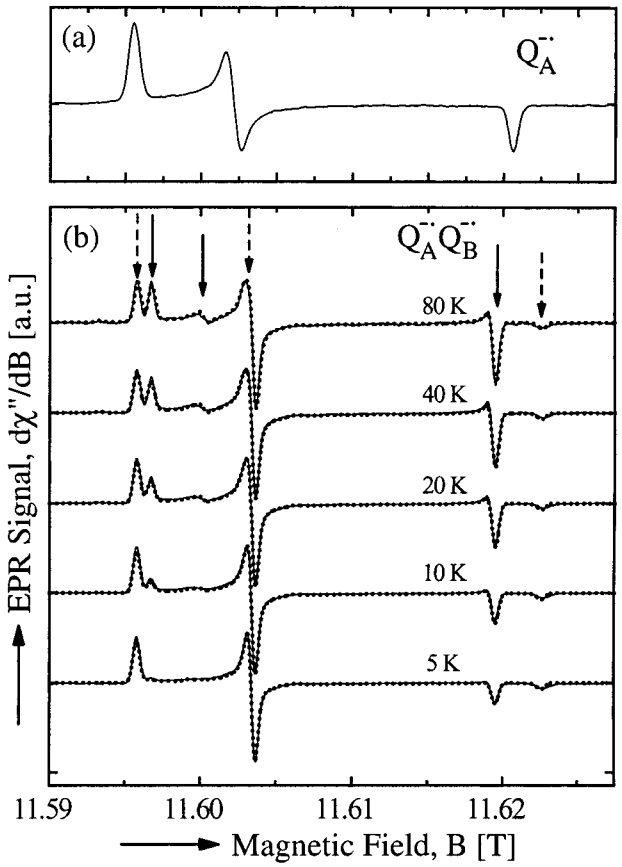

Figure 1. EPR spectra obtained at 326 GHz: (a) Spectrum of $Q_A^{\bullet-}$ at 5 K. The shape of this spectrum does not change with temperature. (b) Spectrum of $Q_A^{\bullet-}Q_B^{\bullet-}$ at 80, 40, 20, 10, and 5 K. Solid lines are experimental results. Dotted lines are simulations performed as explained in the text. From the temperature dependence of the lines indicated by solid arrows, their corresponding transitions can be identified (see text).

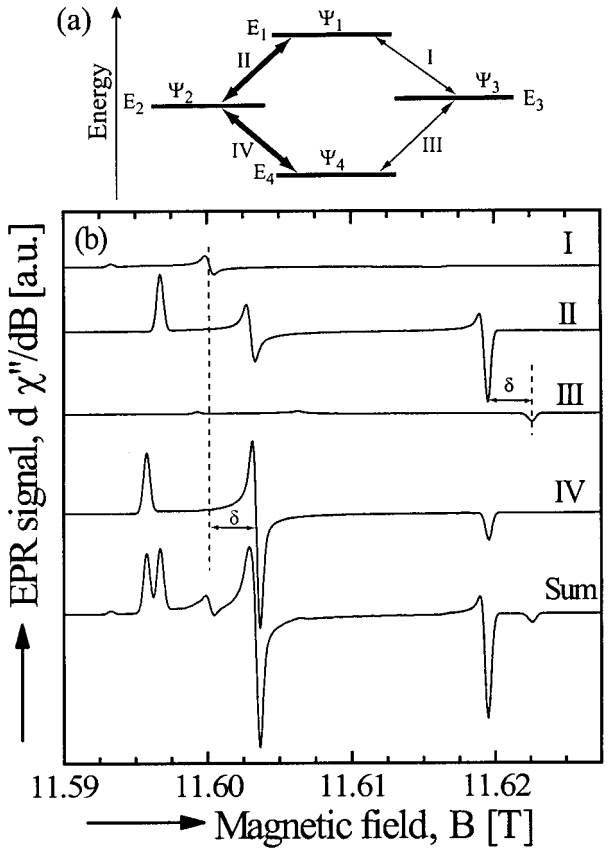

Figure 2. (a) Energy levels E_i of the eigenstates Ψ_i of the biradical $Q_A^{\bullet-}Q_B^{\bullet-}$. The allowed transitions I, ..., IV between these levels are indicated by arrows. Thick arrows indicate transitions with a large transition probability for $J_o < 0$. (b) Simulation of the spectral components corresponding to transitions I, ..., IV of randomly oriented biradicals $Q_A^{\bullet-}Q_B^{\bullet-}$ (i.e., as obtained in frozen solutions). Bottom trace shows the sum of the components without weighting them by the Boltzmann factors. Compare it with the trace at 80 K in Figure 1b. The field splittings "δ" between peaks corresponding to transitions I and IV and transitions II and III may be calculated in the high field approximation from eqs 6.

biradical observed at finite temperatures is the sum of these four contributions, weighted by the respective Boltzmann factors. According to the level scheme in Figure 2a and by neglecting second-order splittings ($E_2 \approx E_3$), the ratio between the populations of states Ψ_2 and Ψ_3 and the population of state Ψ_4 is given by the Boltzmann factor $\exp(-h\nu/kT)$, where $h\nu$ is the Zeeman splitting of the levels. Consequently, the contributions arising from transitions I and II decrease when the temperature is lowered.

Analysis of the Data

To calculate the spin Hamiltonian parameters in eq 1, the EPR data obtained in this work at 326 GHz were analyzed by following the procedure described previously, which does not involve approximations.[1] Briefly, we used the simulated annealing method,[6] together with a routine that calculates the spectrum of a frozen solution to obtain the set of spin-Hamiltonian parameters that gives the best fit to the data. The global annealing fit of the data included the five spectra at temperatures between 5 and 80 K shown in Figure 1b. The asymptotic approach of J_o to its final value in a typical annealing process required many less iterations at 326 GHz than at 94 GHz. This reflects the higher sensitivity of the EPR spectra to the value of J_o at higher frequencies. Accordingly, the dispersion of J_o in a set of 10 independent annealing processes of the data at 326 GHz, is approximately an order of magnitude smaller than at the lower frequencies.[1] Interestingly, the dispersion of the values of E_d obtained in these 10 annealing processes was a factor of 4 larger than the dispersion of the value of E_d calculated from the data at 94 GHz. We attribute the smaller sensitivity to the dipolar interaction of the spectra at 326 GHz compared to 94 GHz to the smaller relative magnitude of E_d compared with the Zeeman interaction at higher frequencies.

The result obtained for the exchange interaction is

$$J_o/h = -82 \pm 3 \text{ MHz}$$

This value agrees within the quoted errors with the result obtained at 94 GHz.[1] However, the uncertainty is approximately an order of magnitude smaller than obtained at lower frequency. The values obtained for the principal components of the **g**-tensors $\mathbf{g}_A$ and $\mathbf{g}_B$, are essentially the same as reported earlier.[1] The structural parameters, contained in the value of E_d, which gives the distance R between radicals, the three Euler angles between the principal axes of $\mathbf{g}_A$ and $\mathbf{g}_B$, and the two angles giving the orientation of the vector ρ in the system of coordinates of $Q_A^{\bullet-}$, also agree within the quoted uncertainties with those reported earlier.[1] The simulations of the spectra calculated with the set of parameters giving the best global fit to the experimental data at different temperatures are shown by dotted lines in Figure 1. The agreement between experiments and simulations is excellent at all temperatures; in fact, it is difficult on the scale of the figure to discern any differences between experiments

and simulations. Figure 2b displays the contributions of transitions I, II, III, and IV to the EPR spectrum of a frozen solution at 326 GHz calculated for the set of spin Hamiltonian parameters obtained from the global fit. Note in Figure 2b that the contributions of the components I and III to the total spectrum at 326 GHz, although smaller than those of the components II and IV, are clearly discernible. The observed changes with temperature of the spectrum of the biradical (Figure 1b) arise from the changes with T of the Boltzmann populations of the four energy states in Figure 2a. According to Figure 2a, the peaks that decrease with T in Figure 1b (see solid arrows) belong to transitions I and II. The summed spectrum in Figure 2b assumes equal Boltzmann factors and corresponds to a high T limit.

The standard high field or low field approximations, valid for $|\Delta g|\mu_B B > |J_o|$ or $|\Delta g|\mu_B B < |J_o|$, respectively,[7] are not strictly valid for the analysis of the spectrum of a frozen solution of the biradical $Q_A^{\bullet-}Q_B^{\bullet-}$ because $\Delta g = g_A(\mathbf{h}) - g_B(\mathbf{h})$ is angular dependent. Consequently, for specific field directions the value of $|\Delta g|$ may be large, small, or even zero. Nevertheless, to help us understand qualitatively the advantages of EPR measurements at higher frequencies, we shall discuss briefly the high field approximation $|\Delta g|\mu_B B > |J_o|$. Series expansions of eqs 2 and 3 in powers of the parameter

$$\epsilon = \frac{J_o + {}^1/_2 d}{\Delta g \mu_B B} \approx \frac{J_o}{\Delta g \mu_B B} \tag{5}$$

show that at high fields ($|\epsilon| < 1$) the line positions B (eqs 2) change as ϵ^2, but the transition probabilities P_j (eqs 3) change linearly with ϵ. Neglecting powers of ϵ larger than quadratic, eqs 2 become

$$g_L \mu_B B_I = h\nu + {}^1/_2(J_o - d(\mathbf{h})) \tag{6a}$$

$$g_S \mu_B B_{II} = h\nu + {}^1/_2(J_o - d(\mathbf{h})) \tag{6b}$$

$$g_S \mu_B B_{III} = h\nu - {}^1/_2(J_o - d(\mathbf{h})) \tag{6c}$$

$$g_L \mu_B B_{IV} = h\nu - {}^1/_2(J_o - d(\mathbf{h})) \tag{6d}$$

where g_L and g_S are the larger, and the smaller g values, respectively ($g_L = g_A$ and $g_S = g_B$ when $g_A > g_B$, or $g_L = g_B$ and $g_S = g_A$ when $g_B > g_A$). Equations 6 show that there are two transitions around the magnetic fields corresponding to g_L and g_S, with a splitting $(J_o - d(\mathbf{h}))$. From the splitting of these pairs of transitions (I and IV or II and III) a value of J_o can be obtained. For high microwave frequency (large B), we expand the transition probabilities (eqs 3) up to first order in ϵ, to obtain

$$P_I = P_{III} \approx 1 - \epsilon \qquad P_{II} = P_{IV} \approx 1 + \epsilon \tag{7}$$

Thus, as $|\epsilon|$ becomes smaller, P_I and P_{III} increase, and transitions I and III become observable. In a frozen sample, the molecules are randomly oriented, and we obtain information about J_o only from biradicals oriented along directions for which $|\epsilon|$ is small ($|\Delta g|\mu_B B > |J_o|$). To increase this fraction of biradicals and obtain a more accurate value of J_o, one can measure the spectrum at higher microwave frequencies. According to eq 6, the distances between pairs of transitions I and IV and transitions II and III are $[(J_o - d(\mathbf{h})]$. However, $d(\mathbf{h})$, in addition to being an order of magnitude smaller than J_o, depends on the orientation of the RCs with respect to the magnetic field and will, therefore, contribute only to the broadening of the line. Thus, the observed transitions occur at $\sim J_o/g\mu_B$. Two of these splittings are indicated by "δ" in Figure 2. Their value is ~3.2 mT, corresponding to ~90 MHz which, considering the limitations of the high field approximation, is in good agreement with the value of 82 MHz obtained from the exact solution.

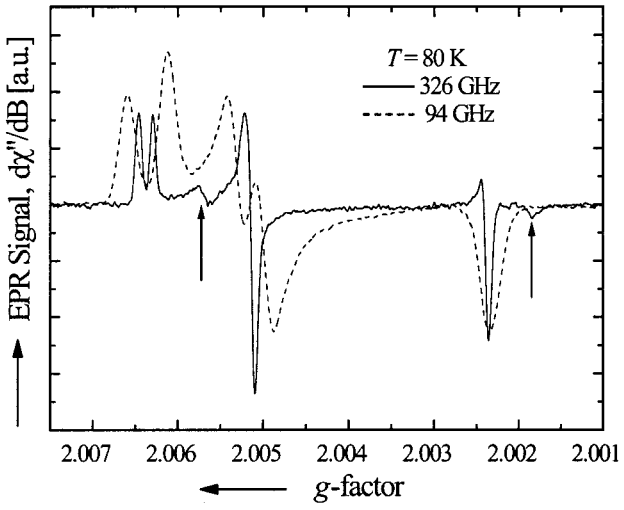

Figure 3. Comparison of the EPR spectra of the biradical $Q_A^{\bullet-}Q_B^{\bullet-}$ at 326 GHz (solid line) with that at 94 GHz (dashed line), both measured at 80 K. Arrows indicate lines that are observed at 326 GHz but are absent in the 94 GHz spectrum. They correspond to transitions I and III (see Figure 2b). These lines contribute strongly to the higher accuracy with which J_o was determined at 326 GHz.

Discussion and Conclusions

There are several motivations to perform EPR experiments at higher frequencies.[8,9] Two important ones are to increase the resolution of the spectra of radicals having a small g-anisotropy and to resolve the spectra of different radicals having similar g-values. These advantages, obtained at high frequencies, have recently being utilized in the study of free radicals formed in photosynthetic systems.[10−15] In the present work we studied the EPR spectra at 326 GHz of the biradical $Q_A^{\bullet-}Q_B^{\bullet-}$, an intermediate state of the photocycle of RCs of *Rb. sphaeroides*. In this four-level system the higher frequency offers the additional advantage of increasing the transition probability of some transitions that were not observed at lower frequencies. This point is illustrated in Figure 3, where we compare the biradical spectra obtained at 94 and 326 GHz, at 80 K. The two lines (see arrows in Figure 3) at $g \sim 2.0056$ and $g \sim 2.0018$ are clearly discernible at 326 GHz but are absent in the 94 GHz spectrum. They arise from transitions III and I, respectively (see Figure 2b). The positions of these peaks are sensitive to the value of J_o and are mainly responsible for the order of magnitude improvement of the accuracy with which J_o was determined in this work. This point is illustrated in Figure 4 which shows a set of simulated spectra at 80 K for different values of J_o, keeping the other spin-Hamiltonian parameters constant and equal to the values used to fit the spectra in Figure 1. The dashed lines in Figure 4 highlight the field shifts of the peaks of the weak transitions as a function of J_o. The experimentally observed spectrum is shown superimposed (dotted) for $J_o/h = -82$ MHz. A similar graph, in which E_d is the variable parameter, shows considerably smaller changes in the spectra, which accounts for the reduced accuracy with which E_d is obtained at 326 GHz. The main reason is that the anisotropy and small value of E_d (compared to J_o) make the spectra at higher frequencies less sensitive to E_d.

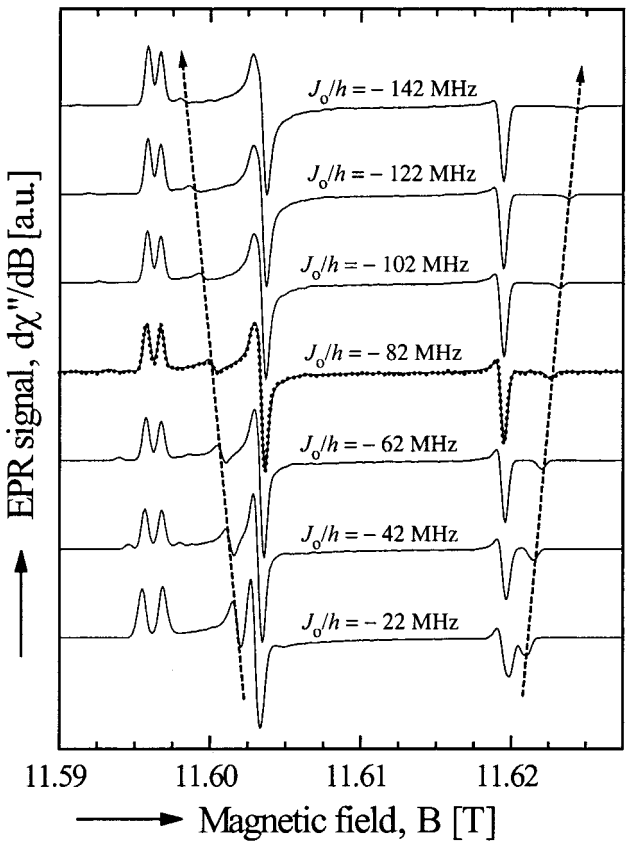

Figure 4. Illustration of the sensitivity of the biradical spectra to the value of J_o/h. Spectra were simulated at 80 K for different values of J_o/h, keeping the other spin-Hamiltonian parameters constant. The two dashed lines highlight the change in positions of two lines for different J_o/h. The spectrum corresponding to $J_o/h = -82$ MHz is compared with the experimental result (dotted) at 80 K.

The value $J_o/h = -82 \pm 3$ MHz obtained in this work is within experimental uncertainty of the previous quoted value of -60 ± 20 MHz.[1] Thus, the estimate of the maximum electron-transfer rate between the semiquinones ($k_{ET}^{max} \approx 10^9$ s^{-1}) derived previously for the value of J_o remains valid.

Acknowledgment. This work was supported by grants from NIH (GM 13191) and NSF (MCB 99-82186). The NHMFL is funded by the NSF under Cooperative Agreement DMR-9527035.

References and Notes

(1) Calvo, R.; Abresch, E. C.; Bittl, R.; Feher, G.; Hofbauer, W.; Isaacson, R. A.; Lubitz, W.; Okamura, M. Y.; Paddock, M. L. *J. Am. Chem. Soc.* **2000**, *122*, 7327.

(2) Okamura, M.; Feher, G. *Annu. Rev. Biochem.* **1992**, *61*, 861.

(3) Stowell, M. H. B.; McPhillips, T. M.; Rees, D. C.; Soltis, S. M.; Abresch, E.; Feher, G. *Science* **1997**, *276*, 812.

(4) Calvo, R.; Isaacson, R. A.; Abresch, E. C.; Paddock, M. L.; Maniero, A.-L.; Saylor, C.; Brunel, L.-C.; Okamura, M. Y.; Feher, G. *Biophys. J.* **2001**, *80* (abstract), 29a.

(5) Hassan, A. K.; Pardi, L. A.; Krzystek, J.; Sienkiewicz, A.; Goy, P.; Rohrer, M.; Brunel, L. C. *J. Mag. Res.* **2000**, *142*, 300.

(6) Kirkpatrick, S.; Gelatt, C. D.; Vecchi, M. P. *Science* **1983**, *220*, 671.

(7) Poole, C. P.; Farach, H. A. *Theory of Magnetic Resonance*, 2nd ed.; Wiley: New York, 1987; Chapters 3−5.

(8) Eaton, S. S.; Eaton, G. R. In *Handbook of Electron Spin Resonance*;Poole, C. P., Farach, H. A., Eds.; AIP Press and Springer-Verlag: New York, 1999; Vol. 2, p 345.

(9) Eaton, G. R.; Eaton, S. S. *Appl. Magn. Reson.* **1999**, *16*, 161.

(10) Bratt, P. J.; Rohrer, M.; Krzystek, J.; Evans, M. C. W.; Brunel, L.-C.; Angerhofer, A. *J. Phys. Chem. B* **1997**, *101*, 9686.

(11) Konovalova, T. A.; Krzystek, J.; Bratt, P. J.; van Tol, J.; Brunel, L.-C.; Kispert, L. D. *J. Phys. Chem. B* **1999**, *103*, 5782.

(12) Bratt, P. J.; Ringus, E.; Hassan, A.; Van Tol, H.; Maniero, A.-L.; Brunel, L.-C.; Rohrer, M.; Bubenzer-Hange, C.; Scheer, H.; Angerhofer, A. *J. Phys. Chem. B* **1999**, *103*, 10973.

(13) Bratt, P. J.; Poluetkov, O. G.; Thurnauer, M. C.; Krzystek, J.; Brunel, L.-C.; Schrier, J.; Hsiao, Y. W.; Zerner, M.; Angerhofer, A. *J. Phys. Chem. B* **2000**, *104*, 6973.

(14) Lakshmi, K. V.; Reifler, M. J.; Brudvig, G. W.; Poluetkov, O. G.; Wagner, A. M.; Thurnauer, M. C. *J. Phys. Chem. B* **2000**, *104*, 10445.

(15) Faller, P.; Rutherford, A. W.; Un, S. *J. Phys. Chem. B* **2000**, *104*, 10960.